International Journal of Control and Automation
Vol. 11, No. 11 (2018), pp.43-56
http//dx.doi.org/10.14257/ijca.2018.11.11.04

Analysis of Exponential and Polynomial Load models using Newton-Raphson Method with Hybrid Power Flow Controller

Seshapalli Sai Ram*, Suresh Babu Daram[1], P.S.Venkataramu[2] and M. S. Nagaraj[3]

**Research Scholar, Dept. of Instrumentation and Control Engineering,
Kalasalingam Academy of Research and Education, Krishnankoil,
[1]Assistant Professor, Dept. of Electrical & Electronics Engineering,
Sree Vidyanikethan Engineering College, Tirupati
[2]Dean Academics, Presidency University, Bengaluru
[3]Professor & Head, Dept. of Electrical & Electronics Engineering
Bapuji Institute of Engineering & Technology, Davangere
seshapallisairam@gmail.com, [1]sureshbabudaram@gmail.com

Abstract

In this paper, exponential and polynomial load model with newton-raphson power flow technique incorporating Hybrid Power Flow Controller (HPFC) is presented. Load model is a mathematical representation of the relationship between voltage and power. The comparison of exponential and polynomial load models without and with HPFC device is also presented. IEEE-14 bus system is used for simulation purpose to show the effectiveness of proposed algorithm.

Keywords: *Static Load Model, Exponential Load Model, Polynomial Load Model, Load Flow Studies, Hybrid Power Flow Controller*

1. Introduction

Load modeling is the study to analyze the accuracy of power system. Load modeling is the mathematical representation of a relationship between power and voltage [1]. The considered active power or reactive power is an output of the load and the voltage magnitude and the voltage angle is the input of the load. The measurement-based approach and the component-based approach are the two basic approaches of load modeling. The measurement-based approach [2] involves direct measurements at different substations and feeders to determine the voltage and frequency characteristics of the active and reactive loads at the point. The data comprises the measurements of voltage and frequency variations, and the corresponding difference in active and reactive power, in real time or to intentional disturbances. The use of continuous field measurements provides real-time information about the status of the system. The operators must take the control decisions. The component-based approach [3] involves the development of a composite load model from the mix of different load classes and the characteristics for each of them. The various load classes are industrial, residential, commercial and other government services. The load composition gives the percentage of each level of load. However, the load mix varies from bus to bus and is dependent on weather and time. Great variety of model structures that have been proposed to build the load model, which can be classified as the physical load model and non-physical load models, or static load model and dynamic load model. The classification of static and dynamic load models is based on the effect of the voltage on the load characteristic. Dynamic load models are more complicated because the response of the

Received (June 17, 2018), Review Result (August 29, 2018), Accepted (September 1, 2018)
* Corresponding Author

ISSN: 2005-4297 IJCA

loads to voltage and frequency variations is a lot faster. However, the detecting of parameters, in this case, can still rely on measured and component-based approaches. More accurate measurements need to be taken as the system's response changes rapidly. The most typical load model is the combination of constant impedance (Z), constant current (I), and constant power (P), often denoted as the ZIP load model. The power flow study is the primary objective of a power system to determine the steady state operating conditions. Steady state operating conditions of a power system can be obtained by calculating active and reactive power flow in the power network and by calculating the magnitudes and angles of the voltage at different nodes of the power network. The main advantage of the Newton Raphson method is its quadratic rate of convergence, which is faster than any other power flow method [4].

The rapid development of power electronics has led to Flexible Ac Transmission Systems (FACTS) devices for utilization in power system [5]. Hybrid Power Flow Controller (HPFC) is one of the latest FACTS devices used as an alternative solution without substantial compromise on versatility [6]. HPFC makes combined use of both variable impedance type and switching converter type FACTS devices. SVC or TCSC is fully utilized with enhanced compensating function.

This paper is organized as follows. Hybrid Power Flow Controller is described in 2. Static load models are described in 3. Constant impedance, constant current, constant power and ZIP load model incorporated to the Newton-Raphson method is described in 4. The proposed algorithm is explained in 5. The case study with simulations results and discussions are given in 6.

2. Hybrid Power Flow Controller

In Hybrid power flow controller (HPFC), two shunt converters (SVC) are connected to a transmission line across a series impedance controller *i.e.*, Thyristor Controlled Series Compensator (TCSC) through coupling transformer [7] [8]. The rating of each shunt converter is half the rated size of total shunt converter. The HPFC has the capability to control real and reactive power flow through the line by varying the magnitude and phase angle of the injected series voltage. It executed by the coordination between the two SVCs and the TCSC. The magnitude of each bus is controlled by controlling the VAR outputs of the shunt converters. Maximum and minimum possible value of injected voltage depends on the maximum and minimum value of TCSC reactance respectively. Figure 1 shows the schematic representation of HPFC. HPFC is modeled by connecting the TCSC in the middle of a line and connecting the MVAR compensator at the adjacent bus. TCSC considered is a variable capacitance. The mathematical model considered for HPFC in given in [9].

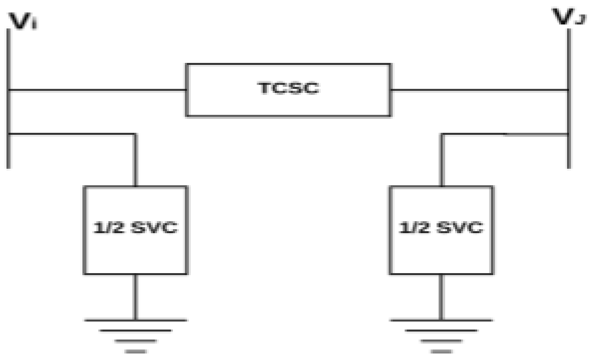

Figure 1. Hybrid Power Flow Controller

The current and the voltage of SVC is given below as in eqn.(1).

$$I_{SVC} = jB_{SVC}V_R \qquad V_{SVC} = V_R = -V_R^2 B_{SVC} \tag{1}$$

B_{SVC} is considered as a static variable and the total SVC susceptance is necessary to maintain the nodal voltage magnitude at the specified bus. If the TCSC is operating in an inductive mode, the values of susceptance is given below as in eqn.(2) and if it is operated in a capacitive mode, the sign is reveresed.

$$B_{ii} = B_{jj} = -\frac{1}{X_{TCSC}} \qquad B_{ij} = B_{ji} = \frac{1}{X_{TCSC}} \tag{2}$$

At bus i, the equations of real and reactive power flow given below as in eqn.(3).

$$P_i = V_i V_j B_{ij} \sin(\theta_i - \theta_j) \qquad Q_i = -V_i^2 B_{ii} - V_i V_j B_{ij} \sin(\theta_i - \theta_j) \tag{3}$$

3. Static Load Models

Different load models [10] would greatly affect power voltage stability analysis. Static load models do not vary with time. In these models, active and reactive power loads are expressed as exponentials and polynomials of voltage and frequency. The different static load models are discussed in following subsections [11,12].

3.1. Exponential Load Model

The exponential load model for real and reactive power at load bus is represented as below.

$$P = P_i \left(\frac{V}{V_0}\right)^a \qquad Q = Q_i \left(\frac{V}{V_0}\right)^b \tag{4}$$

P_i, Q_i, V_i are the initial values of real power, reactive power and voltage at a load bus respectively.

a, b are the load parameters of this model, the value of a and b vary between 0 to 2, for different load models as follows.

If a=b=2, it is constant impedance characteristic

If a=b=1, it is constant current characteristic.

If a=b=0, it is constant power characteristic.

3.1.1. Constant impedance load model:

In the constant impedance load model, power is a function of voltage and changes with the square of voltage. $P_1 + P_2 + P_3 = 1$, $Q_1 + Q_2 + Q_3 = 1$ and $P_2 = Q_2 = P_3 = Q_3 = 0$ $P_1 = Q_1 = 1$. The power values are given below in eqn. (5)

$$P = P_i V^2 \qquad Q = Q_i V^2 \tag{5}$$

3.1.2. Constant current load:

In the constant current load model, power is a function of voltage and is directly proportional to the voltage. $P_1 = Q_1 = P_3 = Q_3 = 0$, $P_1 + P_2 + P_3 = 1$, $Q_1 + Q_2 + Q_3 = 1$ and $P_2 = Q_2 = 1$. The power values are given below in eqn. (6)

$$P = P_i V \qquad Q = Q_i V \tag{6}$$

3.1.3. Constant power load:

In the constant power load model, power is independent of voltage. $P_3 = Q_3 = 1$, $P_2 = Q_2 = P_1 = Q_1 = 0$, $P_1 + P_2 + P_3 = 1$, $Q_1 + Q_2 + Q_3 = 1$. The power values are given below in eqn. (7)

$$P = P_i \qquad\qquad Q = Q_i \tag{7}$$

3.2. Polynomial load model

The polynomial load model is also called as ZIP load model. Z stands for constant impedance, I represent constant current and P refers to constant power. The polynomial model for active and reactive power is as given below in eqn. (8).

$$P = P_i\left[P_1\overline{V}^2 + P_2\overline{V} + P_3\right] \qquad\qquad Q = Q_i\left[Q_1\overline{V}^2 + Q_2\overline{V} + Q_3\right] \tag{8}$$

$$\text{Here } \overline{V} = \frac{V}{V_0} \tag{9}$$

P_i, Q_i and V_0 are the load nominal values of the active, reactive power and voltage.

Most of the loads can be represented as some combination of the ZIP model, with different parameters reflecting the composition. Constant power loads lead to stability problems because there is a tendency to increase the current, in order to maintain constant power even though voltage drops. This can lead to a further drop in the voltage. Constant impedance loads, on the other hand tend to damp voltage oscillations.

4. Polynomial Load Models are incorporated with a Newton-Raphson method

For the analysis of power system, the load models have to be incorporated in any of the analytical technique. In this paper, the polynomial model is incorporated in N-R load flow analysis.

4.1. Constant Impedance (Z) Incorporated With Newton-Raphson Method:

The active and reactive power for constant impedance is given in eqn. (10) as below. The diagonal and off-diagonal elements of active and reactive power for Jacobian matrix are also given.

$$P_Z = \left[\sum_{j=1}^{n} |V_i||V_j||Y_{ij}|\cos(\theta_{ij} - \delta_i + \delta_j)\right] V_i^2 \qquad Q_Z = \left[-\sum_{j=1}^{n} |V_i||V_j||Y_{ij}|\sin(\theta_{ij} - \delta_i + \delta_j)\right] V_i^2 \tag{10}$$

The diagonal and the off-diagonal elements of active power are represented below.

$$\frac{\partial P_Z}{\partial \delta_i} = \sum_{j \neq i} |V_i^3||V_j||Y_{ij}|\sin(\theta_{ij} - \delta_i + \delta_j) \qquad \frac{\partial P_Z}{\partial \delta_j} = -|V_i^3||V_j||Y_{ij}|\sin(\theta_{ij} - \delta_i + \delta_j)\ j \neq i$$

$$\frac{\partial P_Z}{\partial |V_i|} = 4|V_i^3||Y_{ii}|\cos\theta_{ii} + \sum_{j \neq i} 3|V_i^2||V_j||Y_{ij}|\cos(\theta_{ij} - \delta_i + \delta_j) \qquad \frac{\partial P_Z}{\partial |V_j|} = |V_i^3||Y_{ij}|\cos(\theta_{ij} - \delta_i + \delta_j)\ j \neq i$$

The diagonal and the off-diagonal elements of reactive power are represented below.

$$\frac{\partial Q_Z}{\partial \delta_i} = \sum_{j \neq i} |V_i^3||V_j||Yij|\cos(\theta_{ij} - \delta_i + \delta_j) \qquad \frac{\partial Q_Z}{\partial \delta_j} = -|V_i^3||V_j||Y_{ij}|\cos(\theta_{ij} - \delta_i + \delta_j)\ j \neq i$$

$$\frac{\partial Q_Z}{\partial |V_i|} = -4|V_i^3||Y_{ii}|\sin\theta_{ii} - \sum_{j\neq i} 3|V_i^2||V_j||Y_{ij}|\sin(\theta_{ij} - \delta_i + \delta_j) \qquad \frac{\partial Q_Z}{\partial |V_j|} = -|V_i^3||Y_{ij}|\sin(\theta_{ij} - \delta_i + \delta_j)\; j \neq i$$

4.2. Constant Current (I) Incorporated with Newton-Raphson Method:

The active and reactive power for constant current is given in eqn. (11) as below. The diagonal and off-diagonal elements of active and reactive power for Jacobian matrix are also given.

$$P_I = \left[\sum_{j=i}^{n} |V_i||V_j||Y_{ij}|\cos(\theta_{ij} - \delta_i + \delta_j)\right] V_i \quad Q_I = \left[-\sum_{j=i}^{n} |V_i||V_j||Y_{ij}|\sin(\theta_{ij} - \delta_i + \delta_j)\right] V_i \qquad (11)$$

The diagonal and the off-diagonal elements of active power are represented below.

$$\frac{\partial P_I}{\partial \delta_i} = \sum_{j\neq i} |V_i^2||V_j||Y_{ij}|\sin(\theta_{ij} - \delta_i + \delta_j) \qquad \frac{\partial P_I}{\partial \delta_j} = -|V_i^2||V_j||Y_{ij}|\sin(\theta_{ij} - \delta_i + \delta_j)\; j \neq i$$

$$\frac{\partial P_I}{\partial |V_i|} = 3|V_i^2||Y_{ii}|\cos\theta_{ii} + \sum_{j\neq i} 2|V_i||V_j||Y_{ij}|\cos(\theta_{ij} - \delta_i + \delta_j) \qquad \frac{\partial P_I}{\partial |V_j|} = |V_i^2||Y_{ij}|\cos(\theta_{ij} - \delta_i + \delta_j)\; j \neq i$$

The diagonal and the off-diagonal elements of reactive power are represents below.

$$\frac{\partial Q_I}{\partial \delta_i} = \sum_{j\neq i} |V_i^2||V_j||Y_{ij}|\cos(\theta_{ij} - \delta_i + \delta_j) \qquad \frac{\partial Q_I}{\partial \delta_j} = -|V_i^2||V_j||Y_{ij}|\cos(\theta_{ij} - \delta_i + \delta_j)\; j \neq i$$

$$\frac{\partial Q_I}{\partial |V_i|} = 3|V_i^2||Y_{ii}|\sin\theta_{ii} - \sum_{j\neq i} 2|V_i||V_j||Y_{ij}|\sin(\theta_{ij} - \delta_i + \delta_j) \qquad \frac{\partial Q_I}{\partial |V_j|} = -|V_i^2||Y_{ij}|\sin(\theta_{ij} - \delta_i + \delta_j)\; j \neq i$$

4.3. Constant Power (P) Incorporated with Newton-Raphson Method:

The active and reactive power for constant power is given in eqn. (12) as below. The diagonal and off-diagonal elements of active and reactive power for Jacobian matrix are also given.

$$P_P = \left[\sum_{j=i}^{n} |V_i||V_j||Y_{ij}|\cos(\theta_{ij} - \delta_i + \delta_j)\right] \quad Q_P = \left[-\sum_{j=i}^{n} |V_i||V_j||Y_{ij}|\sin(\theta_{ij} - \delta_i + \delta_j)\right] \qquad (12)$$

The diagonal and the off-diagonal elements of active power are represented below.

$$\frac{\partial P_P}{\partial \delta_i} = \sum_{j\neq i} |V_i||V_j||Y_{ij}|\sin(\theta_{ij} - \delta_i + \delta_j) \qquad \frac{\partial P_P}{\partial \delta_j} = -|V_i||V_j||Y_{ij}|\sin(\theta_{ij} - \delta_i + \delta_j)\; j \neq i$$

$$\frac{\partial P_P}{\partial |V_i|} = 2|V_i||Y_{ii}|\cos\theta_{ii} + \sum_{j\neq i} |V_j||Y_{ij}|\cos(\theta_{ij} - \delta_i + \delta_j) \qquad \frac{\partial P_P}{\partial |V_j|} = |V_i||Y_{ij}|\cos(\theta_{ij} - \delta_i + \delta_j)\; j \neq i$$

The diagonal and the off-diagonal elements of reactive power are represented below.

$$\frac{\partial Q_P}{\partial \delta_i} = \sum_{j\neq i} |V_i||V_j||Y_{ij}|\cos(\theta_{ij} - \delta_i + \delta_j) \qquad \frac{\partial Q_P}{\partial \delta_j} = |V_i||V_j||Y_{ij}|\cos(\theta_{ij} - \delta_i + \delta_j)\; j \neq i$$

$$\frac{\partial Q_P}{\partial |V_i|} = -2|V_i||Y_{ii}|\sin\theta_{ii} - \sum_{j\neq i}|V_j||Y_{ij}|\sin(\theta_{ij} - \delta_i + \delta_j) \quad \frac{\partial Q_P}{\partial |V_j|} = -|V_i||Y_{ij}|\sin(\theta_{ij} - \delta_i + \delta_j)\; j \neq i$$

4.4. ZIP Incorporated With Newton-Raphson Method:

The active and reactive power for constant power is given in eqn. (13) as below. The diagonal and off-diagonal elements of active and reactive power for Jacobian matrix are also given.

$$P_{ZIP} = \left[\sum_{j=1}^{n}|V_i||V_j||Y_{ij}|\cos(\theta_{ij} - \delta_i + \delta_j)\right]\left[p_1\bar{V}^2 + p_2\bar{V} + p_3\right] \tag{13}$$

$$P_{ZIP} = P_1\left[\sum_{j=1}^{n}|V_i^3||V_j||Y_{ij}|\cos(\theta_{ij} - \delta_i + \delta_j)\right] + P_2\left[\sum_{j=1}^{n}|V_i^2||V_j||Y_{ij}|\cos(\theta_{ij} - \delta_i + \delta_j)\right] + P_3\left[\sum_{j=1}^{n}|V_i||V_j||Y_{ij}|\cos(\theta_{ij} - \delta_i + \delta_j)\right]$$

$$Q_{ZIP} = \left[-\sum_{j=1}^{n}|V_i||V_j||Y_{ij}|\sin(\theta_{ij} - \delta_i + \delta_j)\right]\left[q_1\bar{V}^2 + q_2\bar{V} + q_3\right]$$

$$Q_{ZIP} = P_1\left[-\sum_{j=1}^{n}|V_i^3||V_j||Y_{ij}|\sin(\theta_{ij} - \delta_i + \delta_j)\right] + P_2\left[-\sum_{j=1}^{n}|V_i^2||V_j||Y_{ij}|\sin(\theta_{ij} - \delta_i + \delta_j)\right] + P_3\left[-\sum_{j=1}^{n}|V_i||V_j||Y_{ij}|\sin(\theta_{ij} - \delta_i + \delta_j)\right]$$

The diagonal and the off-diagonal elements of active power are represented below.

$$\frac{\partial P_{ZIP}}{\partial \delta_i} = \left\{P_1\left[\sum_{j\neq i}|V_i^3||V_j||Y_{ij}|\sin(\theta_{ij} - \delta_i + \delta_j)\right] + P_2\left[\sum_{j\neq i}|V_i^2||V_j||Y_{ij}|\sin(\theta_{ij} - \delta_i + \delta_j)\right] + P_3\left[\sum_{j\neq i}|V_i||V_j||Y_{ij}|\sin(\theta_{ij} - \delta_i + \delta_j)\right]\right\}$$

$$\frac{\partial P_{ZIP}}{\partial \delta_j} = \left\{P_1\left[-|V_i^3||V_j||Y_{ij}|\sin(\theta_{ij} - \delta_i + \delta_j)\right] + P_2\left[-|V_i^2||V_j||Y_{ij}|\sin(\theta_{ij} - \delta_i + \delta_j)\right] + P_3\left[-|V_i||V_j||Y_{ij}|\sin(\theta_{ij} - \delta_i + \delta_j)\right]\right\} j \neq i$$

$$\frac{\partial P_{ZIP}}{\partial |V_i|} = \left\{P_1\left[4|V_i^3||Y_{ii}|\cos\theta_{ii} + \sum_{j\neq i}3|V_i^2||V_j||Y_{ij}|\cos(\theta_{ij} - \delta_i + \delta_j)\right] + \right.$$

$$\left. P_2\left[3|V_i^2||Y_{ii}|\cos\theta_{ii} + \sum_{j\neq i}2|V_i^2||V_j||Y_{ij}|\cos(\theta_{ij} - \delta_i + \delta_j)\right] + P_3\left[2|V_i||Y_{ii}|\cos\theta_{ii} + \sum_{j\neq i}|V_j||Y_{ij}|\cos(\theta_{ij} - \delta_i + \delta_j)\right]\right\}$$

$$\frac{\partial P_{ZIP}}{\partial |V_j|} = \left\{P_1\left[|V_i^3||Y_{ij}|\cos(\theta_{ij} - \delta_i + \delta_j)\right] + P_2\left[|V_i^2||Y_{ij}|\cos(\theta_{ij} - \delta_i + \delta_j)\right] + P_3\left[|V_i||Y_{ij}|\cos(\theta_{ij} - \delta_i + \delta_j)\right]\right\} j \neq i$$

The diagonal and the off-diagonal elements of reactive power are represented below.

$$\frac{\partial Q_{ZIP}}{\partial \delta_i} = \left\{P_1\left[\sum_{j\neq i}|V_i^3||V_j||Y_{ij}|\cos(\theta_{ij} - \delta_i + \delta_j)\right] + P_2\left[\sum_{j\neq i}|V_i^2||V_j||Y_{ij}|\cos(\theta_{ij} - \delta_i + \delta_j)\right] + P_3\left[\sum_{j\neq i}|V_i||V_j||Y_{ij}|\cos(\theta_{ij} - \delta_i + \delta_j)\right]\right\}$$

$$\frac{\partial Q_{ZIP}}{\partial \delta_j} = \left\{P_1\left[-|V_i^3||V_j||Y_{ij}|\cos(\theta_{ij} - \delta_i + \delta_j)\right] + P_2\left[-|V_i^2||V_j||Y_{ij}|\cos(\theta_{ij} - \delta_i + \delta_j)\right] + P_3\left[-|V_i||V_j||Y_{ij}|\cos(\theta_{ij} - \delta_i + \delta_j)\right]\right\}$$

$$\frac{\partial Q_{ZIP}}{\partial |V_i|} = \left\{ P_1 \left[-4|V_i^3||Y_{ii}|\sin\theta_{ii} - \sum_{j\neq i} 3|V_i^2||V_j||Y_{ij}|\sin(\theta_{ij} - \delta_i + \delta_j) \right] + \right.$$

$$\left. P_2 \left[-3|V_i^2||Y_{ii}|\sin\theta_{ii} - \sum_{j\neq i} 2|V_i^2||V_j||Y_{ij}|\sin(\theta_{ij} - \delta_i + \delta_j) \right] + P_3 \left[-2|V_i||Y_{ii}|\sin\theta_{ii} - \sum_{j\neq i} |V_j||Y_{ij}|\sin(\theta_{ij} - \delta_i + \delta_j) \right] \right\}$$

$$\frac{\partial Q_{ZIP}}{\partial |V_j|} = \left\{ P_1 \left[-|V_i^3||Y_{ij}|\sin(\theta_{ij} - \delta_i + \delta_j) \right] + P_2 \left[-|V_i^2||Y_{ij}|\sin(\theta_{ij} - \delta_i + \delta_j) \right] + P_3 \left[-|V_i||Y_{ij}|\sin(\theta_{ij} - \delta_i + \delta_j) \right] \right\} j \neq i$$

From the constant impedance (z), constant current (I), constant power (P), and ZIP incorporated with Newton Raphson method, and we convert equations into the Jacobian matrix. The Jacobian matrix gives the linearized relationship between small changes in voltage angle and voltage magnitude with the small changes in real and reactive power.

$$\begin{bmatrix} \Delta P \\ \Delta Q \end{bmatrix} = \begin{bmatrix} J_1 & J_2 \\ J_3 & J_4 \end{bmatrix} \begin{bmatrix} \Delta\delta \\ \Delta|V| \end{bmatrix}$$

The terms and are the difference between the scheduled and calculated values, known as the power residual given by

$$\Delta P_i^k = P_i^{sch} - P_i^k \qquad \Delta Q_i^k = Q_i^{sch} - Q_i^k \tag{14}$$

The new estimates for bus voltages are

$$\delta_i^{(k+1)} = \delta_i^k + \Delta\delta_i^{(k)} \qquad |V_i^{(k+1)}| = |V_i^{(k)}| + \Delta|V_i^k| \tag{15}$$

5. Proposed Algorithm

The computational methodology has been carried out through the following steps.

Step 1: Read line and bus data of the given system and assumes that system angle, load (MW & MVAR) and generator (MW & MVAR, Q_{min} & Q_{max}) data are constant.

Step 2: Carry out the load flow studies using constant Z load model, constant I load model, constant P load model or ZIP load model one at a time.

Step 3: Calculate voltage magnitudes, voltage angles, active and reactive power flows, number of iterations, power mismatch, for step 2.

Step 4: Compare active and reactive power loss between Z load model with other load models with and without HPFC.

Step 5: Compare active and reactive power loss between I load model with other load models with and without HPFC.

Step 6: Compare active and reactive power loss between P load model with other load models with and without HPFC.

6. Case Study and Results

In this section, numerical results are carried out on IEEE 14-bus system. This system consists of 1-slack bus, 4-generator buses, 9-load buses and 20-transmission lines. The load flow is carried out using Newton-Raphson method for Z-Alone, I-Alone, P-Alone, and ZIP load models. The sum of both active and reactive power parameters is 1.

✓ **Without HPFC**

The results without incorporating HPFC are discussed in different cases as followed:

- Case-1 : Constant Impedance (Z) load model.
- Case-2 : Constant Current (I) load model.
- Case-3 : Constant Power (P) load model.
- Case-4 : All the constant values of Z, I, and P are equal and the value is 0.333.
- Case-5 : All the constant values of Z, I, and P are unequal and the values are 0.50, 0.30, and 0.20 respectively.
- Case-6 : All the constant values of Z, I, and P are unequal and the values are 0.40, 0.35, and 0.25 respectively.

Table 1. Voltage Magnitudes for Different Cases

Bus No.	Case-1	Case-2	Case-3	Case-4	Case-5	Case-6
1	1.06	1.06	1.06	1.06	1.06	1.06
2	1.045	1.045	1.045	1.045	1.045	1.045
3	1.01	1.01	1.01	1.01	1.01	1.01
4	1.015	1.014	1.013	1.014	1.014	1.014
5	1.018	1.017	1.017	1.017	1.018	1.017
6	1.07	1.07	1.07	1.07	1.07	1.07
7	1.047	1.047	1.046	1.046	1.047	1.047
8	1.08	1.08	1.08	1.08	1.08	1.08
9	1.033	1.032	1.031	1.032	1.032	1.032
10	1.032	1.031	1.03	1.031	1.032	1.031
11	1.048	1.047	1.046	1.047	1.047	1.047
12	1.055	1.054	1.053	1.054	1.054	1.054
13	1.048	1.048	1.047	1.048	1.048	1.048
14	1.022	1.021	1.019	1.021	1.021	1.021

The voltage magnitudes and angles for different cases of static load models are shown in Table 1, and Table 2. Compared to various cases, case-1, case-4, and case-5 load model is affecting less on the system. Case-3 load model has effects more on the power system.

Table 2. Voltage Angles for Different Cases

Bus No.	Case-1	Case-2	Case-3	Case-4	Case-5	Case-6
2	-4.784	-4.888	-4.989	-4.893	-4.856	-4.872
3	-12.284	-12.518	-12.749	-12.53	-12.446	-12.481
4	-9.778	-10.013	-10.242	-10.021	-9.94	-9.975
5	-8.34	-8.552	-8.76	-8.559	-8.487	-8.518
6	-13.569	-14.009	-14.447	-14.019	-13.872	-13.938
7	-12.545	-12.895	-13.237	-12.905	-12.787	-12.839
8	-12.545	-12.895	-13.237	-12.905	-12.787	-12.839
9	-14.007	-14.418	-14.82	-14.429	-14.292	-14.353
10	-14.192	-14.618	-15.036	-14.629	-14.486	-14.55
11	-13.986	-14.425	-14.858	-14.435	-14.289	-14.354
12	-14.351	-14.826	-15.297	-14.836	-14.678	-14.749
13	-14.395	-14.865	-15.331	-14.875	-14.719	-14.789
14	-15.155	-15.618	-16.072	-15.63	-15.475	-15.544

Active power flows for different cases of static load models are shown in Table 3. Compared to various cases, case-3 load model is affecting more on the system. Case-5 load model has very low effect on the power system.

Table 3. Active power flows for different cases

Line No.	Case-1	Case-2	Case-3	Case-4	Case-5	Case-6
1	1.5088	1.5403	1.5708	1.5416	1.5306	1.5353
2	0.7202	0.7378	0.7551	0.7384	0.7324	0.735
3	0.7105	0.7223	0.734	0.7229	0.7186	0.7204
4	0.5322	0.546	0.5594	0.5464	0.5417	0.5438
5	0.394	0.4057	0.4173	0.406	0.4021	0.4038
6	0.2388	0.2369	0.2353	0.2372	0.2375	0.2373
7	0.5848	0.593	0.6006	0.5935	0.5905	0.5917
8	0.2509	0.2609	0.2707	0.261	0.2578	0.2593
9	0.1435	0.1491	0.1546	0.1492	0.1474	0.1482
10	0.4227	0.4407	0.4589	0.4409	0.4351	0.4378
11	0.0801	0.0816	0.0829	0.0817	0.0812	0.0814
12	0.074	0.0773	0.0806	0.0774	0.0763	0.0768
13	0.1707	0.1771	0.1834	0.1772	0.1751	0.1761
15	0.2509	0.2609	0.2707	0.261	0.2578	0.2593
16	0.0378	0.0408	0.0439	0.0408	0.0398	0.0403
17	0.0802	0.0833	0.0864	0.0833	0.0823	0.0828
18	0.0471	0.047	0.0466	0.0471	0.0471	0.0471
19	0.0185	0.0187	0.0188	0.0188	0.0187	0.0187
20	0.0641	0.0645	0.0646	0.0646	0.0645	0.0645

Table 4. Reactive Power Flows for Different Cases

Line No.	Case-1	Case-2	Case-3	Case-4	Case-5	Case-6
1	0.2527	0.2653	0.2776	0.2658	0.2614	0.2633
2	0.0481	0.0501	0.0522	0.0501	0.0495	0.0498
2	0.0378	0.0366	0.0354	0.0365	0.037	0.0368
4	0.0078	0.0093	0.0108	0.0093	0.0088	0.009
5	0.0254	0.0269	0.0285	0.0269	0.0264	0.0267
6	0.0628	0.0669	0.071	0.0671	0.0657	0.0663
7	0.1118	0.1138	0.1157	0.1139	0.1132	0.1135
8	0.0547	0.0551	0.0556	0.0551	0.055	0.0551
9	0.0321	0.0333	0.0345	0.0334	0.033	0.0332
10	0.1164	0.1144	0.1126	0.1144	0.115	0.1147
11	0.0817	0.0853	0.089	0.0854	0.0842	0.0848
12	0.0287	0.0302	0.0318	0.0302	0.0297	0.03
13	0.0916	0.0957	0.0998	0.0958	0.0944	0.095
14	0.2002	0.2053	0.2103	0.2055	0.2037	0.2045
15	0.1394	0.1438	0.148	0.1439	0.1425	0.1431
16	0.0075	0.0083	0.0092	0.0083	0.0081	0.0082
17	0.0041	0.0037	0.0032	0.0037	0.0038	0.0038
18	0.063	0.0657	0.0684	0.0658	0.0649	0.0653
19	0.0129	0.0135	0.0141	0.0135	0.0133	0.0134
20	0.0474	0.0491	0.0508	0.0492	0.0486	0.0489

Reactive power flows for different cases of static load models are shown in Table 4. Compared to various cases, case-3, case-2 and case-4 load models are affecting more on the system. Case-1, case-5 load model has very low effect on the power system.

✓ **With HPFC**

HPFC is connected in bus-4 to bus-5 line. The initial capacitance of the TCSC is 0.015 and to avoid over compensation, the working range of TCSC is choosing between -0.015 to 0.015 of line reactance. The value considered for SVC is 20 MVAR.

The results with incorporating HPFC are discussed in different cases as followed:

Case-1 : Constant Impedance (Z) load model with HPFC.
Case-2 : Constant Current (I) load model with HPFC.
Case-3 : Constant Power (P) load model with HPFC.
Case-4 : With HPFC of the constant values of Z, I, and P are equal and the value is 0.333.
Case-5 : With HPFC of the constant values of Z, I, and P are unequal and the values are 0.50, 0.30, and 0.20 respectively.
Case-6 : With HPFC of the constant values of Z, I, and P are unequal and the values are 0.40, 0.35, and 0.25 respectively.

The voltage magnitudes for different cases of static load models are shown in Table 5. Compared to various cases, case-1, case-4, and case-5 load model is affecting less on the system. Case-3 load model has effect more on the power system.

Table 5. Load Bus Voltage Magnitude for IEEE-14 Bus System

Bus No.	Case-1	Case-2	Case-3	Case-4	Case-5	Case-6
4	1.019	1.018	1.018	1.018	1.018	1.018
5	1.028	1.027	1.028	1.027	1.028	1.027
7	1.05	1.049	1.053	1.049	1.049	1.049
9	1.036	1.035	1.037	1.035	1.035	1.035
10	1.035	1.034	1.035	1.034	1.034	1.034
11	1.049	1.048	1.049	1.048	1.049	1.049
12	1.057	1.057	1.056	1.057	1.057	1.057
13	1.049	1.048	1.048	1.048	1.049	1.048
14	1.025	1.023	1.023	1.023	1.023	1.023

The voltage angles for different cases of static load models are shown in Table 6. Compared to various cases, case-3 load model is affecting more on the system. Case-1, case-2 and case-5 load model has very low effect on the power system.

Table 6. Load Bus Voltage Angles for IEEE-14 Bus System

Bus No.	Case-1	Case-2	Case-3	Case-4	Case-5	Case-6
4	-9.014	-9.257	-9.511	-9.265	-9.182	-9.218
5	-8.856	-9.096	-9.338	-9.103	-9.022	-9.058
7	-11.966	-12.332	-12.708	-12.341	-12.219	-12.274
9	-13.527	-13.959	-14.397	-13.969	-13.825	-13.89
10	-13.807	-14.257	-14.705	-14.267	-14.118	-14.185
11	-13.826	-14.29	-14.74	-14.3	-14.146	-14.215
12	-14.035	-14.523	-14.981	-14.532	-14.371	-14.443
13	-14.277	-14.77	-15.239	-14.78	-14.617	-14.69
14	-14.826	-15.313	-15.786	-15.324	-15.162	-15.235

Active power flows for different cases of static load models are shown in Table 7. Compared to various cases, case-3load model is affecting more on the system. Case-5 load model has very low effect on the power system.

Table 7. Active Power Flows for Different Cases

Line No.	Case-1	Case-2	Case-3	Case-4	Case-5	Case-6
1	1.461675	1.495204	1.527664	1.496492	1.484894	1.48989
2	0.758571	0.778638	0.798511	0.779245	0.772441	0.775433
3	0.677658	0.689422	0.700901	0.690056	0.685801	0.687563
4	0.467786	0.481642	0.495728	0.481976	0.477347	0.479414
5	0.446576	0.460275	0.473314	0.460588	0.456025	0.45807
6	0.270586	0.268707	0.267175	0.269026	0.269319	0.269044
7	0.705009	0.71621	0.728868	0.716872	0.712855	0.714511
8	0.269317	0.280124	0.29229	0.280267	0.276771	0.27838
9	0.154127	0.160256	0.166809	0.160336	0.158355	0.159267
10	0.390074	0.40845	0.424531	0.408589	0.402654	0.405407
11	0.058847	0.060282	0.060221	0.060356	0.059877	0.060084
12	0.087397	0.091609	0.095314	0.09164	0.090282	0.090913
13	0.146005	0.151886	0.156997	0.151975	0.150067	0.150942
14	1.46E-15	1.28E-15	1.58E-15	1.21E-15	2.78E-17	4.23E-16
15	0.269317	0.280124	0.29229	0.280267	0.276771	0.27838
16	0.058276	0.061614	0.066169	0.061609	0.060543	0.061046
17	0.090379	0.09368	0.09793	0.093726	0.092655	0.093145
18	0.026185	0.025959	0.024321	0.026023	0.026079	0.026036
19	0.031959	0.032919	0.033273	0.032951	0.032635	0.032775
20	0.053345	0.053872	0.053006	0.053956	0.053762	0.05383

Reactive power flows for different cases of static load models are shown in Table 8. Compared to various cases, case-3, case-2 and case-4 load models are affecting more on the system. Case-1, case-5 load model has very low effect on the power system.

Table 8. Reactive Power Flows for Different Cases

Line No	Case-1	Case-2	Case-3	Case-4	Case-5	Case-6
1	0.23384	0.24721	0.260206	0.247725	0.243093	0.245087
2	0.061688	0.000296	0.075384	0.000277	0.065091	7.77E-05
3	0.04127	0.040002	0.038791	0.039934	0.040389	0.040201
4	-0.00026	0.000501	0.006899	0.000505	0.000161	0.000323
5	0.040721	0.042435	0.048945	0.042522	0.041914	0.042169
6	0.05174	0.055559	0.054426	0.055784	0.054382	0.054955
7	0.183834	0.186778	0.202393	0.186993	0.185875	0.186316
8	0.046566	0.046743	0.065827	0.046738	0.046671	0.046701
9	0.035207	0.036731	0.034015	0.036762	0.036268	0.036493
10	0.160598	0.159175	0.161722	0.159158	0.159611	0.159401
11	0.083693	0.087579	0.084967	0.087628	0.086365	0.086946
12	0.022916	0.0242	0.024624	0.024205	0.023791	0.023985
13	0.097039	0.101515	0.102684	0.101566	0.100115	0.100785
14	0.185466	0.190753	0.231396	0.19086	0.189125	0.189912
15	0.133705	0.138514	0.15763	0.138621	0.137052	0.137764
16	0.01053	0.011406	0.00624	0.011408	0.011122	0.011255
17	0.002942	0.002538	0.005991	0.002551	0.002677	0.002614
18	0.065524	0.068446	0.065083	0.068487	0.067536	0.067972
19	0.007728	0.008095	0.007583	0.0081	0.00798	0.008035
20	0.048392	0.05028	0.048054	0.050316	0.049699	0.049979

✓ Comparisons

The comparison of exponential load model and polynomial load models are discussed. Polynomial load model is the composite load model. Figure 2 shows total active power loss for different static load model with and without HPFC. Compared to different cases, case-3 load model is affecting more on the system. Case-1 load model has very low effect on the power system. The system comparatively secure with HPFC.

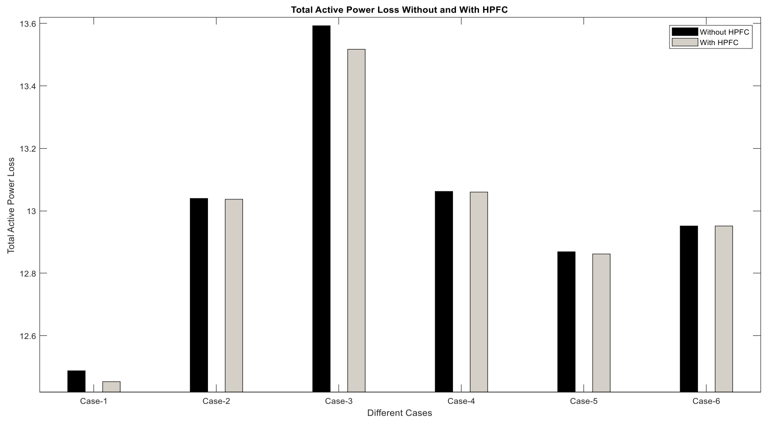

Figure 2. Active Power loss for Different Cases

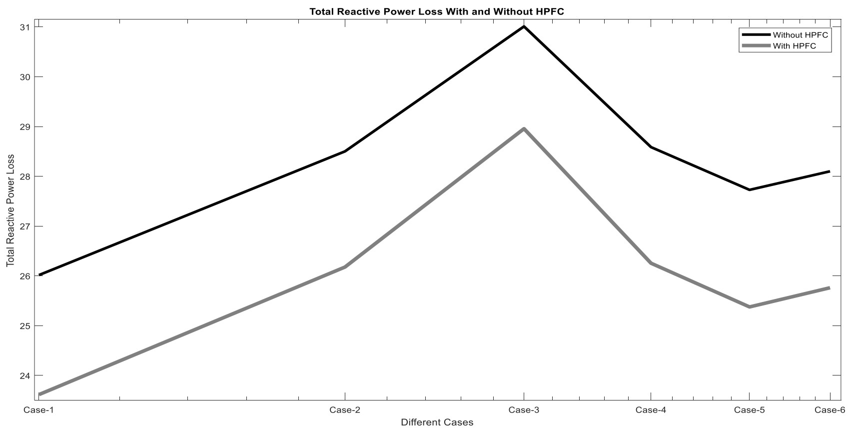

Figure 3. Reactive Power Loss for Different Cases

7. Conclusion

The mathematical model for exponential and polynomial load model with newton-raphson power flow technique is developed. The combination of the constant values reflects in the system. The comparison of different load models has been studied. Among all the load models, constant power is more effective in the power system. Hybrid Power Flow Controller is incorporated in power system. When the system reaches to emergency state of operation, it can be switched to restorative state by allocating HPFC at proper location. The system is more stable with HPFC compared to without HPFC in the system. The loss in the system has been reduced with HPFC.

Acknowledgment

The authors are thankful to Dr. T. Nageswara Prasad, HOD and advanced renewable research lab, Department of EEE Sree Vidyanikethan Engineering College, Tirupati for the constant encouragement and providing the facilities to complete this work.

References

[1] Cheng-Hong Gu, Qian Ai, Jiayi WU, "A Study of Effect of Different Static Load Models and System Operating Constraints on Static Voltage Stability", proceeding of 5th WSEAS/IASME international Conference on system theory and scientific computation, pp. 44-49, Sept. 2005.
[2] A. Borghetti, R. Caldon, A. Mari and C. A. Nucci, "On Dynamic Load Models for Voltage Stability Studies", IEEE Transactions on Power Syst., Vol. 12, Nov. 1997.
[3] B.-K. Choi, H. D. Chiang, Y. Li, Y. T. Chen, D. H. Huang, and M. G. Lauby, "Development of composite load models of power systems using on-line measurement data", Journal of Electrical Engineering and Technology, vol. 1, no. 2, pp. 161–169, 2006.
[4] Salah kamel and mohamed k.el-nemr, "Hybrid Power And Current Mismatches Newton-raphson Load-flow Analysis For Solving Power Systems With Voltage Controlled Devices", International Middle East Power System Conference (MEPCON'10), pp.1-6, Dec. 2010.
[5] Hingorani, Narain G., Laszlo Gyugyi, "Understanding FACTS", IEEE press, First edition, 2001.
[6] Bebic, Jovan Z., Peter W. Lehn, and M. R. Iravani. "The hybrid power flow controller-a new concept for flexible AC transmission", IEEE Power Engineering Society General Meeting, oct.2006.
[7] Merritt, N. R. & Chatterjee, D. "Performance improvement of power systems using Hybrid Power Flow Controller", International Conference on Power and Energy Systems (ICPS), 2011 (pp. 1-6). Dec. 2011.
[8] Tamimi, B., Canizares, C., & Battistelli, C. "Hybrid Power Flow Controller Steady-State Modeling, Control, and Practical Application", IEEE Transactions on Power Systems, pp. 1483-1492. 2017.
[9] Seshapalli Sai Ram, Suresh Babu Daram, P.S.Venkataramu, M.S.Nagaraj, "Comparative Study of SVC, TCSC and HPFC using ZIP Load Modeling", International Journal of Electronics, Electrical and Computational System IJEECS, Volume 7, Issue 4, April 2018.
[10] M. Sadeghi and G. A. Sarvi, "Determination of ZIP parameters with least squares optimization method", in Elect. Power Energy Conf., pp. 1–6, 2009.
[11] Seshapalli Sai Ram, Suresh Babu Daram, P.S.Venkataramu, M.S.Nagaraj, "Analysis of ZIP Load Modeling in Power Transmission System", International Journal of Control and Automation, Vol. 11, No. 7, pp.11-24, 2018.
[12] Seshapalli Sai Ram, Suresh Babu Daram, P.S.Venkataramu and M.S.Nagaraj, "Comparative Study of SVC, TCSC, and HPFC using ZIP Load Modeling," International Journal of Electronics, Electrical and Computational System, Volume 7, Issue 4, April 2018 , pp. 595-611.

Authors

Seshapalli Sairam was born in West Godavari (A.P), India in 1995. He received his B.Tech in Electrical and Electronics Engineering from Ramachandra College of Engineering in 2016 and M.Tech in Electrical Power Systems from Sree Vidyanikethan Engineering College, Tirupati. He is a Research scholar in the Department of Instrumentation and Control Engineering from Kalasalingam Academy of Research and Education (India). He has published 3 national/ International journal / conference papers.

His area of research includes load modeling, Micro-grid, and security analysis.

Suresh Babu Daram was born in Vijayawada (A.P), India in 1985. He received his B.Tech in Electrical & Electronics engineering from JNTU in 2006 and M.Tech degree in Power Systems Engg from ANU, in 2009. He is a Research Scholar in the Department of Electrical & Electronics Engineering at the Visvesvaraya Technological University Belgaum (India).

He was Assistant Professor in the Dept. of Electrical & Electronics at GGITM Bhopal from 2009-2015. Currently he is Asst. Prof in Dept. of Electrical & Electronics, Sree Vidyanikethan Engineering College, Tirupati (A.P), India. He has published 32 national/ International journal / conference papers. His research interests include energy management systems, power system optimization, and voltage instability studies incorporating FACTS controllers and security analysis.

Mr. Suresh is a member of IEEE, AMIE (India), IAENG, CSTA, IACSIT, IRED and Student Member-ASTM.

P. S. Venkataramu was born in India on June 20, 1961. He received his Graduation in Electrical Engineering from the Institute of Engineers (India), M. Tech degree in Power Systems from Mysore University (India) and Ph.D. in 2007 from Visvesvaraya Technological University, Belgaum (India).

He was employed as an Electrical Engineer in the Goa state Electricity Department and worked for 15 years in various capacities. He was primarily involved in carrying power system operational and planning studies for the regional grid system. He was also a visiting faculty in the Goa college of Engineering. From 1997 to 2007, he worked as a faculty in various positions at School of Electrical Sciences, Vellore Institute of Technology, Vellore, India. From 2007 to 2015 he was a Professor in Electrical Engineering Department and Principal of Gyan Ganga Institute of Technology and Management, Bhopal (India). He was Dean -Internal Quality at REVA University, Bangalore from 2015 to 2018. He is currently Dean Academics, Presidency University, Bengaluru. He has several national and international publications. His research interest includes AI application to power system and distribution system automation.

Dr. P. S. Venkataramu is a Fellow of the Institution of Engineers (India), Indian society for technical education, and System society of India.

M. S. Nagaraj completed his B.E degree in Electrical & Electronics in the year 1986 from Government BDT College of Engineering, Davangere. Master Engineering, Mysore in the year 1991 & 2007 respectively.

He has teaching experience of 25 years in Under Graduate College. At present, he is working as Professor & Head in the Department of Electrical & Electronics Engg, BIET, Davangere. He has published several research papers in national/ International journal /conference papers. His research interest includes AI application to the power system.

Dr. M. S. Nagaraj is a member of Indian Society for Technical Education and Institution of Engineers (India).